



ELSEVIER

Available online at www.sciencedirect.com ScienceDirectCommunications in
Nonlinear Science and
Numerical Simulation

Communications in Nonlinear Science and Numerical Simulation xxx (2007) xxx–xxx

www.elsevier.com/locate/cnsns

Dynamics of three coupled limit cycle oscillators with application to artificial intelligence

Lee Mendelowitz, Anael Verdugo, Richard Rand *

Department of Theoretical and Applied Mechanics, Cornell University, Ithaca, NY 14853, United States

Received 31 July 2007; received in revised form 26 August 2007; accepted 26 August 2007

Abstract

We study a system of three limit cycle oscillators which exhibits two stable steady states. The system is modeled by both phase-only oscillators and by van der Pol oscillators. We obtain and compare the existence, stability and bifurcation of the steady states in these two models. This work is motivated by application to the design of a machine which can make decisions by identifying a given initial condition with its associated steady state.

© 2007 Elsevier B.V. All rights reserved.

PACS: 02.30.Hq; 07.05.Mh; 07.10.Cm

Keywords: MEMS oscillators; Associative memory; Phase-locked motion; Coupled oscillators

1. Introduction

The idea of this work is that a dynamical system which has multiple stable steady states can be used as a decision-making device by basing decisions on the system's steady-state behavior. That is, given an input signal (thought of as an initial condition for the dynamical system), a machine must decide to which of several distinct possible outcomes the input signal corresponds. This is accomplished by allowing the system to come to steady state and identifying the input signal with the steady state. Thus all initial conditions lying in the basin of attraction of a given steady state will be identified with that steady state. Such systems have been identified as being analogous to brain models involving associative memory [1].

This idea is particularly applicable to MEMS/NEMS technology. In a recent paper, Zalalutdinov et al. [2] treated a system of 400 NEMS oscillators and showed how the steady-state dynamics were affected by changes in coupling strength and by differences in individual frequencies (mistuning). Simulations of a system of 20×20 identical phase-only oscillators with nearest-neighbor coupling has been shown to include a wide variety of stable steady states, including, in addition to the in-phase mode, spiral wave patterns which appear to be

* Corresponding author. Tel.: +1 607 255 7145; fax: +1 607 255 2011.
E-mail address: rrand1@tcny.rr.com (R. Rand).

centered at an arbitrary point, and more complicated patterns which appear to involve several spiral waves, each centered at a different point [3]. In an effort to investigate the simplest system of coupled oscillators which exhibits multiple steady states, Rand and Wong [3] studied a system of four coupled phase-only oscillators and showed that if some of the coupling coefficients were chosen to be negative (called “inhibitory” coupling in the biological literature [4]) the system could exhibit a continuum of stable steady states.

In the present paper we study an even simpler system, one consisting of three limit cycle oscillators, which we show is able to exhibit two stable steady states. We begin by discussing phase-only models of three coupled oscillators. We focus on a particularly simple system, call it S_1 , which has the desirable property of exhibiting two stable steady states. Then we investigate the robustness of this property, that is, we ask for which system parameters does the model S_1 continue to exhibit two stable steady states. Finally we present a more realistic model consisting of three van der Pol oscillators, call it S_2 , which is shown to correspond to our phase-only system S_1 . We study the model S_2 using both perturbation methods and direct numerical integration, and we show that it also exhibits two stable steady states.

2. Three coupled phase-only oscillators

Following Kuramoto [5] we take the coupling function in a system of coupled phase-only oscillators as a sine function. Then the most general system of three phase-only oscillators is given by the equations:

$$\dot{\theta}_1 = \omega_1 + \alpha_{21} \sin(\theta_2 - \theta_1) + \alpha_{31} \sin(\theta_3 - \theta_1) \quad (1)$$

$$\dot{\theta}_2 = \omega_2 + \alpha_{12} \sin(\theta_1 - \theta_2) + \alpha_{32} \sin(\theta_3 - \theta_2) \quad (2)$$

$$\dot{\theta}_3 = \omega_3 + \alpha_{13} \sin(\theta_1 - \theta_3) + \alpha_{23} \sin(\theta_2 - \theta_3) \quad (3)$$

where θ_i is the phase of oscillator i , ω_i is the uncoupled frequency of oscillator i , and the coupling coefficient α_{ij} represents the effect of oscillator i on oscillator j . See Fig. 1. This system has been previously studied in [4] in the case that $\alpha_{21} = \alpha_{12} = \alpha_{32} = \alpha_{23} = \alpha$ and $\alpha_{31} = \alpha_{13} = \beta$.

Eqs. (1)–(3) may be simplified by defining the phase differences $\phi_1 = \theta_1 - \theta_3$ and $\phi_2 = \theta_2 - \theta_3$, giving the two equations:

$$\dot{\phi}_1 = \Omega_1 - (\alpha_{13} + \alpha_{31}) \sin \phi_1 - \alpha_{23} \sin \phi_2 - \alpha_{21} \sin(\phi_1 - \phi_2) \quad (4)$$

$$\dot{\phi}_2 = \Omega_2 - \alpha_{13} \sin \phi_1 - (\alpha_{23} + \alpha_{32}) \sin \phi_2 + \alpha_{12} \sin(\phi_1 - \phi_2) \quad (5)$$

where $\Omega_1 = \omega_1 - \omega_3$ and $\Omega_2 = \omega_2 - \omega_3$. Note that an equilibrium point in Eqs. (4) and (5) corresponds to a phase-locked motion in Eqs. (1)–(3). Note also that Eqs. (4) and (5) represent a flow on a torus $S \times S$, that is, the phase variables ϕ_i are defined mod 2π .

An interesting question to ask about the system of Eqs. (4) and (5) is what is the maximum number of equilibrium points that such a system can exhibit? This question may be addressed by computing the condition on the parameters such that a bifurcation involving a change in the number of equilibria occurs. This condition was obtained by using the computer algebra system MACSYMA/MAXIMA, as follows: We begin by trig expanding the right-hand sides of Eqs. (4) and (5), giving

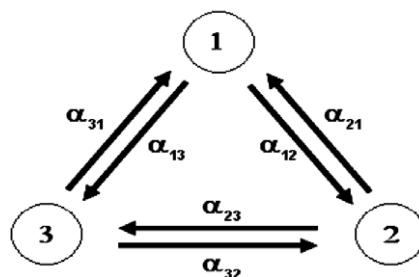


Fig. 1. Schematic representation of the three phase-only oscillator model.

$$\Omega_1 - (\alpha_{13} + \alpha_{31})u - \alpha_{23}v - \alpha_{21}\left(u\sqrt{1-v^2} - v\sqrt{1-u^2}\right) = 0 \quad (6)$$

$$\Omega_2 - \alpha_{13}u - (\alpha_{23} + \alpha_{32})v + \alpha_{12}\left(u\sqrt{1-v^2} - v\sqrt{1-u^2}\right) = 0 \quad (7)$$

where we have abbreviated $u = \sin \phi_1$ and $v = \sin \phi_2$, whereupon $\cos \phi_1 = \sqrt{1-u^2}$ and $\cos \phi_2 = \sqrt{1-v^2}$. Next we wish to eliminate v from Eqs. (6) and (7). We can derive an expression for v in terms of u by multiplying (6) by α_{12}/α_{21} and adding the result to Eq. (7). This yields

$$v = c_1u + c_2 \quad (8)$$

where c_1 and c_2 are listed in the appendix. Now Eq. (8) could be substituted into Eq. (6), giving an equation on u only, but the resulting equation would involve square roots and would thus be awkward to manipulate algebraically. Instead, we first solve Eq. (6) for $\sqrt{1-u^2}$ and square both sides, thereby eliminating the term $\sqrt{1-u^2}$. The resulting equation will still depend on $\sqrt{1-v^2}$, so we solve it for $\sqrt{1-v^2}$ and again square both sides, yielding a polynomial on u and v , call it

$$f(u, v) = 0 \quad (9)$$

which turns out to have 68 terms. Now we may substitute Eq. (8) into the resulting equation, yielding a polynomial equation

$$f(u, c_1u + c_2) \equiv F(u) = 0 \quad (10)$$

on u alone. This turns out to be a 6th degree polynomial in u which has 739 terms, and which may be written in the abbreviated form:

$$F(u) = K_6u^6 + K_5u^5 + K_4u^4 + K_3u^3 + K_2u^2 + K_1u + K_0 = 0 \quad (11)$$

Each of the terms K_i turns out to be an 8th degree polynomial in the parameters α_{ij} and Ω_i . These are too long to list even in the appendix, but some additional information about them is given there.

Now we may obtain a condition for a bifurcation in which the number of equilibria to Eqs. (4) and (5) changes by algebraically eliminating u from the two equations $F(u) = 0$ and $dF/du = 0$, where $F(u)$ is the polynomial in Eq. (11). This is accomplished in MACSYMA/MAXIMA by using the command ELIMINATE. The result is a sum of 246 terms, each of which is a monomial of degree 10 in the K_i , that is, each term is of the form

$$A(K_0)^{i_0}(K_1)^{i_1}(K_2)^{i_2}(K_3)^{i_3}(K_4)^{i_4}(K_5)^{i_5}(K_6)^{i_6} \quad (12)$$

where $\sum_{j=0}^6 i_j = 10$ and where A is an integer. For example a typical term is $1700K_0K_1^4K_4K_5^2K_6^2$.

We thus have derived a closed form expression for the desired bifurcation condition. This condition represents a codimension one manifold in the eight-dimensional parameter space α_{ij}, Ω_i . However, we find that the expression itself contains so many terms that we are at a loss to be able to use it for the general system of Eqs. (4) and (5). However, it may be used to find bifurcations for various classes of subsystems which involve fewer parameters. For example, for the system studied in [4], for which $\alpha_{21} = \alpha_{12} = \alpha_{32} = \alpha_{23} = \alpha$, $\alpha_{31} = \alpha_{13} = \beta$ and $\Omega_1 = \Omega_2 = 0$, we obtain $\beta = \pm\alpha/2$, which agrees with the result given in [4]. Inspection of the flows of Eqs. (4) and (5) in each of the bifurcation regions shows that there are up to six equilibria for this system, again in agreement with [4].

An algebraic simplification occurs whenever one or more of the parameters is zero. We are thus led to classify the system in Fig. 1 according to which coupling parameters are zero. We find that there are seven distinct cases, omitting trivial repeats due to permuting subscripts. See Fig. 2.

Since the key equation (11) involves $u = \sin \phi_1$, it might be supposed that additional bifurcations occur when the roots of $F(u)$ pass through $u = \pm 1$. Substituting $u = \pm 1$ into Eq. (11) gives a condition on the system parameters which is a squared quantity, and the roots u which lie in the neighborhood of this condition always satisfy the equation $|u| < 1$. Thus the condition $u = \pm 1$ does not represent a bifurcation for Eqs. (4) and (5).

Let us return now to the question as to what is the maximum number of equilibria a system described by Eqs. (4) and (5) can exhibit. Since Eq. (11) is a 6th degree polynomial in u , it cannot possess more than 6 real

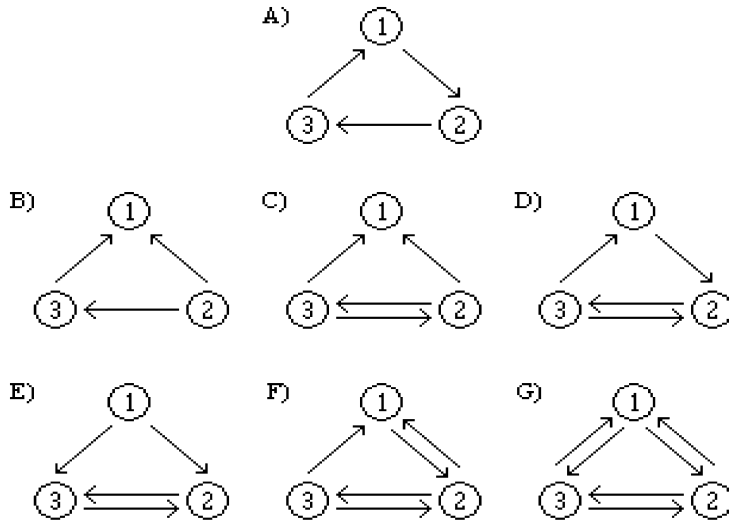


Fig. 2. The systems shown in Fig. 1 may be classified according to which coefficients α_{ij} are zero. There are seven distinct cases, omitting trivial repeats due to permuting subscripts.

roots. Corresponding to each root $u = \sin \phi_1$, Eq. (8) gives a corresponding value for $v = \sin \phi_2$. Substituting these two expressions into the right hand side of Eq. (4), we may solve for $\sin(\phi_1 - \phi_2)$:

$$\sin(\phi_1 - \phi_2) = \frac{\Omega_1 - (\alpha_{13} + \alpha_{31})u - \alpha_{23}v}{\alpha_{21}} \tag{13}$$

Due to the multivaluedness of the arcsine function, the two expressions for $u = \sin \phi_1$ and $v = \sin \phi_2$ yield four possible values for ϕ_1 and ϕ_2 . We list these below, together with the corresponding value of $\sin(\phi_1 - \phi_2)$:

$$(\phi_1^*, \phi_2^*) \quad \sin(\phi_1^* - \phi_2^*) \tag{14}$$

$$(\pi - \phi_1^*, \phi_2^*) \quad \sin(\phi_1^* + \phi_2^*) \tag{15}$$

$$(\phi_1^*, \pi - \phi_2^*) \quad -\sin(\phi_1^* + \phi_2^*) \tag{16}$$

$$(\pi - \phi_1^*, \pi - \phi_2^*) \quad -\sin(\phi_1^* - \phi_2^*) \tag{17}$$

If we suppose that Eq. (14) satisfies Eq. (13), then the other three values for ϕ_1 and ϕ_2 will not do so for general values of the parameters because $\sin(\phi_1^* - \phi_2^*)$ does not in general equal $\pm \sin(\phi_1^* + \phi_2^*)$ or $-\sin(\phi_1^* - \phi_2^*)$. Thus in this general case, each root u of the 6th degree polynomial equation (11) provides a single acceptable equilibrium point (ϕ_1^*, ϕ_2^*) .

Now consider the special case for which $\sin(\phi_1^* - \phi_2^*) = -\sin(\phi_1^* - \phi_2^*)$, i.e. for which $\sin(\phi_1 - \phi_2) = 0$. Here $\phi_1 - \phi_2$ must equal either 0 or π , which gives that $v = \sin \phi_2 = \pm \sin \phi_1 = \pm u$. Then it turns out that substituting $v = \pm u$ into the polynomial $f(u,v) = 0$ of Eq. (9) gives a 6th degree polynomial $F(u) = 0$ which always has a double root. Thus in this case we would get no more than five roots u , one of which gives both (ϕ_1^*, ϕ_2^*) and $(\pi - \phi_1^*, \pi - \phi_2^*)$, and the other four of which each gives a unique equilibrium (ϕ_1^*, ϕ_2^*) , for a total of not more than six equilibria. The other special cases in which $\sin(\phi_1^* - \phi_2^*) = \pm \sin(\phi_1^* + \phi_2^*)$ can be handled similarly.

Thus we have proved that the system of three coupled phase-only oscillators described by Eqs. (4) and (5) cannot exhibit more than six equilibria.

3. An example with two stable equilibria

In the present paper we study case A (see Fig. 2) where each oscillator is coupled to one other oscillator with identical inhibitory coupling, that is, $\alpha_{21} = \alpha_{32} = \alpha_{13} = 0$ and $\alpha_{31} = \alpha_{12} = \alpha_{23} = -\alpha$, where $\alpha > 0$. Substituting the latter into Eqs. (1)–(3) yields

$$\dot{\theta}_1 = \omega_1 - \alpha \sin(\theta_3 - \theta_1) \tag{18}$$

$$\dot{\theta}_2 = \omega_2 - \alpha \sin(\theta_1 - \theta_2) \tag{19}$$

$$\dot{\theta}_3 = \omega_3 - \alpha \sin(\theta_2 - \theta_3) \tag{20}$$

and Eqs. (4) and (5) become

$$\dot{\phi}_1 = \Omega_1 + \alpha \sin \phi_1 + \alpha \sin \phi_2 \tag{21}$$

$$\dot{\phi}_2 = \Omega_2 + \alpha \sin \phi_2 - \alpha \sin(\phi_1 - \phi_2) \tag{22}$$

Before proceeding with the analysis of this system, we rescale time with $\tau = \alpha t$ and define

$$W_i = \frac{\Omega_i}{\alpha} = \frac{\omega_i - \omega_3}{\alpha}, \quad i = 1, 2 \tag{23}$$

which gives the following form of Eqs. (21) and (22):

$$\phi_1' = W_1 + \sin \phi_1 + \sin \phi_2 \tag{24}$$

$$\phi_2' = W_2 + \sin \phi_2 - \sin(\phi_1 - \phi_2) \tag{25}$$

We note that the system of Eqs. (24) and (25) is invariant under the two transformations T_1, T_2 :

$$T_1 : W_i \rightarrow -W_i, \quad \phi_i \rightarrow -\phi_i \tag{26}$$

$$T_2 : W_1 \rightarrow W_2, W_2 \rightarrow W_2 - W_1, \quad \phi_1 \rightarrow \phi_2, \phi_2 \rightarrow \phi_2 - \phi_1 \tag{27}$$

We may now apply the results of our computer algebra analysis presented in the previous section to Eqs. (24) and (25) in order to obtain the bifurcation curves in the W_1 – W_2 plane which separate regions containing a distinct number of equilibria. We obtain

$$\begin{aligned} &64W_2^{10} - 320W_1W_2^9 + 16W_1^4W_2^8 + 584W_1^2W_2^8 - 399W_2^8 - 64W_1^5W_2^7 - 416W_1^3W_2^7 + 1596W_1W_2^7 \\ &+ 96W_1^6W_2^6 - 128W_1^4W_2^6 - 934W_1^2W_2^6 + 840W_2^6 - 64W_1^7W_2^5 + 496W_1^5W_2^5 - 2784W_1^3W_2^5 \\ &- 2520W_1W_2^5 + 16W_1^8W_2^4 - 128W_1^6W_2^4 + 4643W_1^4W_2^4 - 772W_1^2W_2^4 - 766W_2^4 - 416W_1^7W_2^3 \\ &- 2784W_1^5W_2^3 + 5744W_1^3W_2^3 + 1532W_1W_2^3 + 584W_1^8W_2^2 - 934W_1^6W_2^2 - 772W_1^4W_2^2 - 2298W_1^2W_2^2 \\ &+ 288W_2^2 - 320W_1^9W_2 + 1596W_1^7W_2 - 2520W_1^5W_2 + 1532W_1^3W_2 - 288W_1W_2 + 64W_1^{10} - 399W_1^8 \\ &+ 840W_1^6 - 766W_1^4 + 288W_1^2 - 27 = 0 \end{aligned} \tag{28}$$

A graph of this equation is displayed in Fig. 3. Note that the symmetries in this graph follow from the invariances T_1 and T_2 of Eqs. (26) and (27). The integers in Fig. 3 represent the number of equilibria found in systems lying in each region, a result obtained by numerically integrating Eqs. (24) and (25).

For the application to artificial intelligence, we are interested in those systems which have two stable steady states. These correspond to the systems which lie in the central region of Fig. 3, all of which contain 6 equilibria. The origin $W_1 = W_2 = 0$ represents the ideal case for which all three oscillators have the same uncoupled frequency, $\omega_1 = \omega_2 = \omega_3$, cf. Eqs. (18)–(20), and for this case we have the following equilibria (ϕ_1, ϕ_2) :

$$\text{Source} = \{(0, 0)\} \tag{29}$$

$$\text{Saddles} = \{(0, \pi), (\pi, 0), (\pi, \pi)\} \tag{30}$$

$$\text{Sinks} = \left\{ \left(\frac{2\pi}{3}, \frac{4\pi}{3} \right), \left(\frac{4\pi}{3}, \frac{2\pi}{3} \right) \right\} \tag{31}$$

See Fig. 4 which shows a phase portrait for this case.

The nature of the stable steady states (31) may be understood by substituting (31) back into Eqs. (18)–(20) with $\omega_1 = \omega_2 = \omega_3 = \omega$. In the case of the first of (31), θ_2 is a third of a cycle ahead of θ_1 , which is itself a third of a cycle ahead of θ_3 . Thus in this case the motion represents a uniform wave moving around the three oscillators of Fig. 1 in a counterclockwise direction. For this case we find that all three oscillators operate with a common frequency of $\omega + \frac{\sqrt{3}}{2}\alpha$. The opposite is the case for the second of (31), which corresponds to a wave

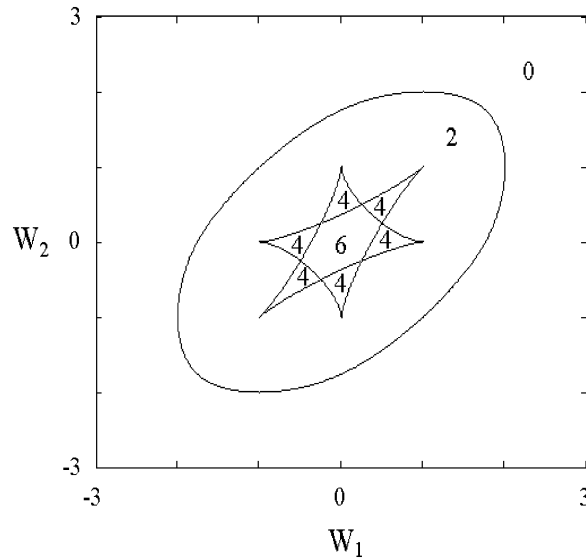


Fig. 3. The bifurcation set (28) for Eqs. (24) and (25). The number of equilibria in each region are shown as integers.

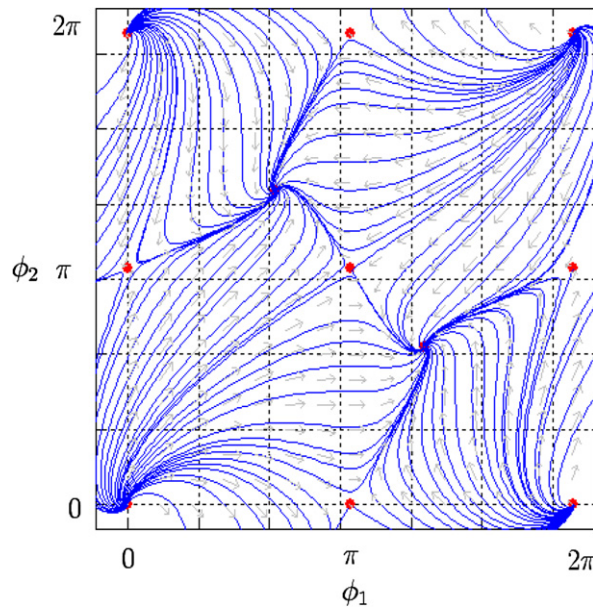


Fig. 4. Phase portrait for Eqs. (24) and (25) with $W_1 = W_2 = 0$. The flow has one source, three saddles and two sinks.

moving around Fig. 1 in a clockwise direction. The common frequency for this case is found to be $\omega - \frac{\sqrt{3}}{2}\alpha$. Such rotating waves have been observed in an experimental study involving time delay [6].

These rotating waves have also been noted in a study involving three identical oscillators [7]. In a real system, however, it will be impossible to make the three frequencies ω_i equal. The extent to which the three oscillators can be detuned and still exhibit the desired property of two stable steady states is given by the frequency-difference pairs (W_1, W_2) which lie in the central region of Fig. 3. See Fig. 5 which shows an enlargement of Fig. 3 in which the shaded region represents the robustness of the two stable steady states. From Fig. 5 we note that the boundaries of the shaded region are nearly straight lines. See Fig. 6 where a comparison is made between the boundaries given by the bifurcation Eq. (28) and straight lines through the vertices of the shaded

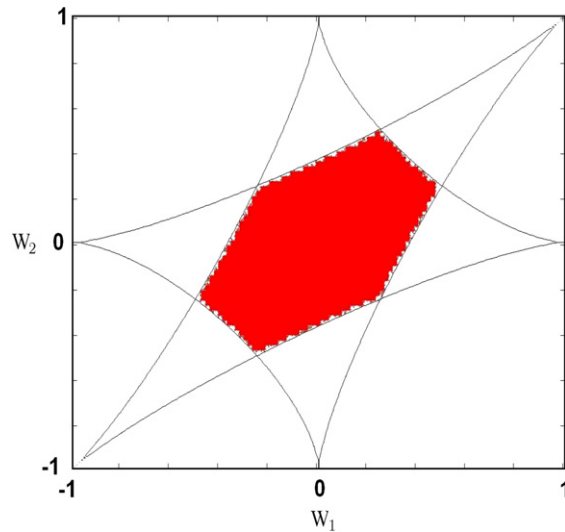


Fig. 5. Enlargement of Fig. 3 in which the shaded region represents detunings for which the system of Eqs. (18)–(20) exhibits two stable steady states.

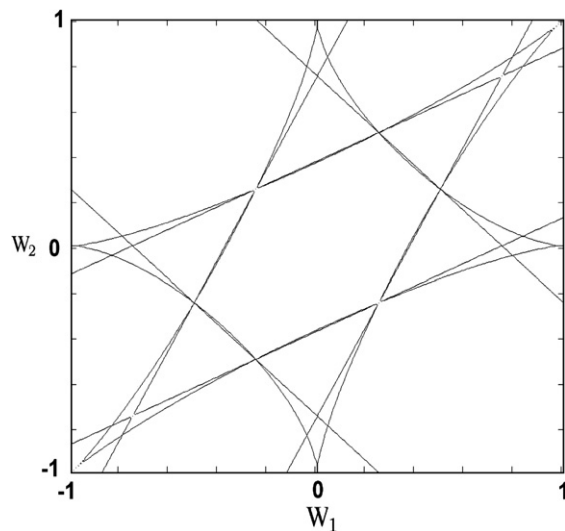


Fig. 6. Comparison of the boundaries of the shaded region in Fig. 5, given by the bifurcation equation (28), with the straight lines listed in Eqs. (32)–(34).

region. Thus a person designing a device based on this system could use the straight lines instead of the bifurcation equation (28) to determine possible detunings. The equations of the six straight lines are

$$4W_1 - 8W_2 = \pm 3 \quad (32)$$

$$8W_1 - 4W_2 = \pm 3 \quad (33)$$

$$4W_1 + 4W_2 = \pm 3 \quad (34)$$

A natural question which arises when considering the two-dimensional example system of Eqs. (24) and (25) is: Are Hopf bifurcations possible for this system? The answer is no, as we show as follows. The linearization of Eqs. (24) and (25) about an equilibrium point (ϕ_1, ϕ_2) gives the Jacobian matrix J :

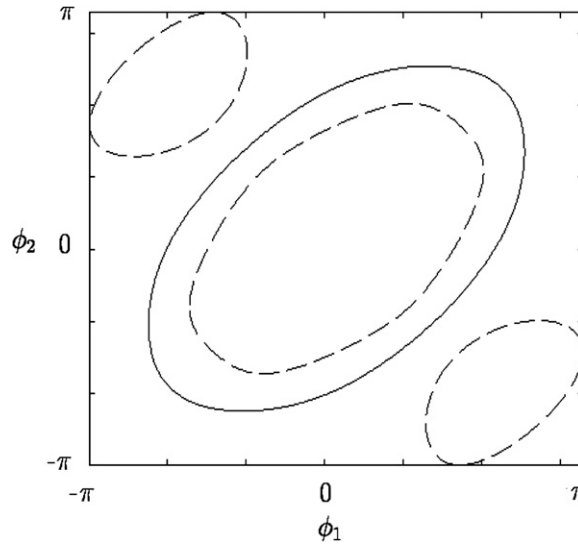


Fig. 7. Diagram proving that Eqs. (24) and (25) cannot exhibit a Hopf bifurcation. Solid line represents $\text{trace}(J) = 0$. Dashed lines represent $\text{determinant}(J) = 0$. The regions inside the closed dashed curves represent $\text{determinant}(J) > 0$. There are no points (ϕ_1, ϕ_2) for which both $\text{trace}(J) = 0$ and $\text{determinant}(J) > 0$.

$$J = \begin{pmatrix} \cos \phi_1 & \cos \phi_2 \\ -\cos(\phi_2 - \phi_1) & \cos(\phi_2 - \phi_1) + \cos \phi_2 \end{pmatrix} \quad (35)$$

The condition for a Hopf bifurcation in which a limit cycle is generically born is well known to be [10,12]:

$$\text{trace}(J) = \cos(\phi_2 - \phi_1) + \cos \phi_2 + \cos \phi_1 = 0 \quad (36)$$

$$\text{determinant}(J) = (\cos \phi_2 + \cos \phi_1) \cos(\phi_2 - \phi_1) + \cos \phi_1 \cos \phi_2 > 0 \quad (37)$$

Fig. 7 displays a plot of these two conditions, demonstrating that there are no points (ϕ_1, ϕ_2) for which both conditions hold.

4. Three coupled van der Pol oscillators

Although phase-only oscillator models embody the essential features governing the dynamics of coupled oscillators, they omit reference to the vibration amplitudes which are present in more realistic models of oscillators. Thus we are led to ask whether the kind of behavior which we have seen in the preceding section, i.e., a system of three oscillators which exhibits two stable steady states, also holds when phase-only oscillators are replaced by more realistic oscillator models. For this purpose we choose van der Pol oscillators because they are a common paradigm for limit cycle oscillators.

Consider the following system of three coupled van der Pol oscillators:

$$\ddot{x} + \omega_1^2 x - \epsilon(1 - x^2)\dot{x} = -2\epsilon\alpha\dot{z} \quad (38)$$

$$\ddot{y} + \omega_2^2 y - \epsilon(1 - y^2)\dot{y} = -2\epsilon\alpha\dot{x} \quad (39)$$

$$\ddot{z} + \omega_3^2 z - \epsilon(1 - z^2)\dot{z} = -2\epsilon\alpha\dot{y} \quad (40)$$

We investigate the dynamics of this system in two ways. Firstly, we use perturbations, valid for small ϵ , in the case that the three frequencies ω_i are equal, to derive a slow flow which we show is analogous to our ideal phase-only model of Eqs. (24) and (25). Then secondly, we use numerical integration, in the case that the three frequencies are not equal, to show that this model exhibits two stable steady states.

Thus assuming that $\omega_1 = \omega_2 = \omega_3 = \omega$, we use the two variable expansion method (also known as multiple scales) to obtain a slow flow. (See [8–11] for examples of this method.) Working to $O(\epsilon)$, we set $\xi = t, \eta = \epsilon t$,

and expand $x = x_0 + \epsilon x_1$, $y = y_0 + \epsilon y_1$, and $z = z_0 + \epsilon z_1$. Substituting the latter into (38)–(40), expanding, collecting ϵ like terms, and neglecting $O(\epsilon^2)$ terms gives

$$\frac{\partial^2 x_0}{\partial \xi^2} + \omega^2 x_0 = 0, \quad \frac{\partial^2 y_0}{\partial \xi^2} + \omega^2 y_0 = 0, \quad \frac{\partial^2 z_0}{\partial \xi^2} + \omega^2 z_0 = 0 \tag{41}$$

$$\frac{\partial^2 x_1}{\partial \xi^2} + \omega^2 x_1 = -2 \frac{\partial^2 x_0}{\partial \xi \partial \eta} + (1 - x_0^2) \frac{\partial x_0}{\partial \xi} - 2\alpha \frac{\partial z_0}{\partial \xi} \tag{42}$$

$$\frac{\partial^2 y_1}{\partial \xi^2} + \omega^2 y_1 = -2 \frac{\partial^2 y_0}{\partial \xi \partial \eta} + (1 - y_0^2) \frac{\partial y_0}{\partial \xi} - 2\alpha \frac{\partial x_0}{\partial \xi} \tag{43}$$

$$\frac{\partial^2 z_1}{\partial \xi^2} + \omega^2 z_1 = -2 \frac{\partial^2 z_0}{\partial \xi \partial \eta} + (1 - z_0^2) \frac{\partial z_0}{\partial \xi} - 2\alpha \frac{\partial y_0}{\partial \xi} \tag{44}$$

Taking the general solutions to Eq. (41) in the form

$$x_0 = R_1(\eta) \cos(\omega \xi - \psi_1(\eta)), \quad y_0 = R_2(\eta) \cos(\omega \xi - \psi_2(\eta)), \quad z_0 = R_3(\eta) \cos(\omega \xi - \psi_3(\eta)) \tag{45}$$

and substituting them into (42)–(44), then removing resonant terms, we obtain the following slow flow:

$$\psi_1' = -\alpha \frac{R_3}{R_1} \sin(\psi_3 - \psi_1) \tag{46}$$

$$\psi_2' = -\alpha \frac{R_1}{R_2} \sin(\psi_1 - \psi_2) \tag{47}$$

$$\psi_3' = -\alpha \frac{R_2}{R_3} \sin(\psi_2 - \psi_3) \tag{48}$$

$$R_1' = \frac{R_1}{2} - \frac{R_1^3}{8} - \alpha R_3 \cos(\psi_3 - \psi_1) \tag{49}$$

$$R_2' = \frac{R_2}{2} - \frac{R_2^3}{8} - \alpha R_1 \cos(\psi_1 - \psi_2) \tag{50}$$

$$R_3' = \frac{R_3}{2} - \frac{R_3^3}{8} - \alpha R_2 \cos(\psi_2 - \psi_3) \tag{51}$$

where primes represent differentiation with respect to slow time η . Letting $\phi_1 = \psi_1 - \psi_3$ and $\phi_2 = \psi_2 - \psi_3$, we may reduce the six-dimensional system (46)–(51) to the following five-dimensional system:

$$\phi_1' = \alpha \frac{R_3}{R_1} \sin \phi_1 + \alpha \frac{R_2}{R_3} \sin \phi_2 \tag{52}$$

$$\phi_2' = \alpha \frac{R_2}{R_3} \sin \phi_2 - \alpha \frac{R_1}{R_2} \sin(\phi_1 - \phi_2) \tag{53}$$

$$R_1' = \frac{R_1}{2} - \frac{R_1^3}{8} - \alpha R_3 \cos \phi_1 \tag{54}$$

$$R_2' = \frac{R_2}{2} - \frac{R_2^3}{8} - \alpha R_1 \cos(\phi_1 - \phi_2) \tag{55}$$

$$R_3' = \frac{R_3}{2} - \frac{R_3^3}{8} - \alpha R_2 \cos \phi_2 \tag{56}$$

where these equations are defined on the space $S \times S \times R^+ \times R^+ \times R^+$, that is, the ϕ_i are taken mod 2π and the R_j are non-negative. Note the similarity between the phase equations (52) and (53) and the phase-only model given by Eqs. (21) and (22). We see that if α is neglected in the three R_i equations (54)–(56), then we obtain $R_1 = R_2 = R_3 = 2$. When this is substituted into the phase equations (52) and (53), we recover the phase-only equations (21) and (22), which we have shown exhibit two stable steady states. But what if we don't neglect α in the three R_i equations? Does this system still exhibit two stable steady states?

To find out, we search for steady states, $(\phi_1^*, \phi_2^*, R_1^*, R_2^*, R_3^*)$, by setting $\phi_i' = R_i' = 0$ in (52)–(56) and solving for ϕ_i^* and R_i^* . We find the following equilibrium points:

$$\phi_1^* = \phi_2^* = 0, \quad R_1^* = R_2^* = R_3^* = 2\sqrt{1-2\alpha} \tag{57}$$

$$\phi_1^* = 0, \quad \phi_2^* = \pi, \quad R_1^* = R_3^* = -2\sqrt{1-2\alpha}, \quad R_2^* = 2\sqrt{1-2\alpha} \tag{58}$$

$$\phi_1^* = \pi, \quad \phi_2^* = 0, \quad R_1^* = -2\sqrt{1-2\alpha}, \quad R_2^* = R_3^* = 2\sqrt{1-2\alpha} \tag{59}$$

$$\phi_1^* = \pi, \quad \phi_2^* = \pi, \quad R_1^* = R_2^* = 2\sqrt{1-2\alpha}, \quad R_3^* = -2\sqrt{1-2\alpha} \tag{60}$$

$$\phi_1^* = \frac{2\pi}{3}, \quad \phi_2^* = \frac{4\pi}{3}, \quad R_1^* = R_2^* = R_3^* = 2\sqrt{1+\alpha} \tag{61}$$

$$\phi_1^* = \frac{4\pi}{3}, \quad \phi_2^* = \frac{2\pi}{3}, \quad R_1^* = R_2^* = R_3^* = 2\sqrt{1+\alpha} \tag{62}$$

Since the equilibria (58)–(60) corresponding to negative values of R_i are not physically relevant, we discount them. Also the equilibrium (57) does not exist for $\alpha > 1/2$. So for $0 < \alpha < 1/2$ we are left with three steady states

$$(0, 0, 2\sqrt{1-2\alpha}, 2\sqrt{1-2\alpha}, 2\sqrt{1-2\alpha}) \tag{63}$$

$$\left(\frac{2\pi}{3}, \frac{4\pi}{3}, 2\sqrt{1+\alpha}, 2\sqrt{1+\alpha}, 2\sqrt{1+\alpha}\right) \tag{64}$$

$$\left(\frac{4\pi}{3}, \frac{2\pi}{3}, 2\sqrt{1+\alpha}, 2\sqrt{1+\alpha}, 2\sqrt{1+\alpha}\right) \tag{65}$$

We may determine the stability of these equilibria by computing the eigenvalues of the Jacobian matrix of Eqs. (52)–(56). It turns out that (63) is unstable for $0 < \alpha < 1/2$ and that both (64) and (65) are stable for $\alpha > 0$. Details are given in the appendix.

Since the five-dimensional slow flow of Eqs. (52)–(56) has two stable equilibria, it is of interest to know what dynamical entity serves as the separatrix or basin boundary separating the basins of attraction of the two stable equilibria. In order to find out, we numerically integrated the rectangular coordinate form of the six-dimensional slow flow of Eqs. (46)–(51), defined by the polar coordinate transformation:

$$a_i = R_i \cos \psi_i, \quad b_i = R_i \sin \psi_i, \quad i = 1, 2, 3 \tag{66}$$

The reason for using the a_i – b_i equations instead of the R_i – ψ_i equations is that, as we show below, the separatrix consists of a periodic motion which periodically visits each of the regions $R_1 = 0$, $R_2 = 0$, and $R_3 = 0$, all of which are singularities in the ψ_i (Eqs. (46)–(48)).

$$\frac{da_1}{d\eta} = -a_3\alpha - \frac{a_1 b_1^2}{8} - \frac{a_1^3}{8} + \frac{a_1}{2} \tag{67}$$

$$\frac{db_1}{d\eta} = -b_3\alpha - \frac{b_1^3}{8} - \frac{a_1^2 b_1}{8} + \frac{b_1}{2} \tag{68}$$

$$\frac{da_2}{d\eta} = -a_1\alpha - \frac{a_2 b_2^2}{8} - \frac{a_2^3}{8} + \frac{a_2}{2} \tag{69}$$

$$\frac{db_2}{d\eta} = -b_1\alpha - \frac{b_2^3}{8} - \frac{a_2^2 b_2}{8} + \frac{b_2}{2} \tag{70}$$

$$\frac{da_3}{d\eta} = -a_2\alpha - \frac{a_3 b_3^2}{8} - \frac{a_3^3}{8} + \frac{a_3}{2} \tag{71}$$

$$\frac{db_3}{d\eta} = -b_2\alpha - \frac{b_3^3}{8} - \frac{a_3^2 b_3}{8} + \frac{b_3}{2} \tag{72}$$

By trial and error we find that the initial condition $a_1 = 2$, $b_1 = 0.001$, $a_2 = 2$, $b_2 = 0.001$, $a_3 = 0.001$, $b_3 = 0$, nearly lies on the stable manifold of an unstable periodic motion in the case that $\alpha = 1$. See Fig. 8, which, using Eq. (66), shows the time history of R_1 , R_2 and R_3 for this initial condition. After spending some time near the unstable periodic motion, the trajectory approaches one of the equilibria equations 64 and 65 for which $R_1 = R_2 = R_3 = 2\sqrt{1+\alpha} = 2\sqrt{2} \approx 2.82$.

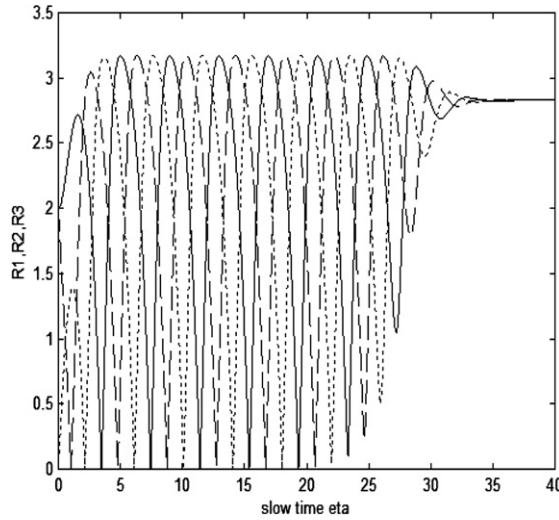


Fig. 8. Numerical integration of slow flow of Eqs. (67)–(72) for initial conditions $a_1 = 2, b_1 = 0.001, a_2 = 2, b_2 = 0.001, a_3 = 0.001, b_3 = 0$. The trajectory comes close to an unstable periodic motion which is the basin boundary between the two stable steady states (64) and (65), but eventually approaches a stable equilibrium. Solid line = R_1 , dashed line = R_2 , and dotted line = R_3 .

We have shown that the five-dimensional slow flow of Eqs. (52)–(56) corresponding to $\omega_1 = \omega_2 = \omega_3 = \omega$, exhibits two stable equilibria. We now consider the stability of these equilibria when the three uncoupled frequencies ω_i are not equal. We set $\omega_i = \omega + \epsilon\delta_i$ for $i = 1, 2, 3$, and we define $\Delta_j = \delta_j - \delta_3$ for $j = 1, 2$. Then Eqs. (52) and (53) become

$$\phi_1' = -\Delta_1 + \alpha \frac{R_3}{R_1} \sin \phi_1 + \alpha \frac{R_2}{R_3} \sin \phi_2 \tag{73}$$

$$\phi_2' = -\Delta_2 + \alpha \frac{R_2}{R_3} \sin \phi_2 - \alpha \frac{R_1}{R_2} \sin(\phi_1 - \phi_2) \tag{74}$$

while Eqs. (54)–(56) are unchanged. We used the bifurcation program AUTO to determine for which detuning parameters (Δ_1, Δ_2) the equilibria equations (64) and (65) are stable, respectively. The results are that both equilibria lose their stability in supercritical Hopf bifurcations, see Fig. 9. Each of the oval-shaped curves

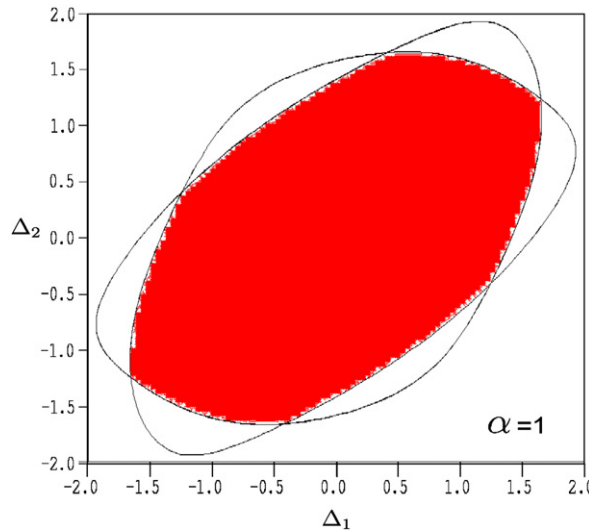


Fig. 9. Shaded region represents systems in which both of the equilibria (64) and (65) are stable. Each of the oval-shaped curves represents the locus of supercritical Hopfs for one of these equilibria.

in Fig. 9 represents the locus of Hopfs for one of the equilibria. The shaded region in Fig. 9 represents the range of detuning parameters for which the system (52)–(56) exhibits two stable equilibria. In the neighborhood of the outside of the shaded region, at least one, and at some points both, of the equilibria have given birth to stable limit cycles. In view of Eq. (45), such limit cycles correspond to quasiperiodic motions in the original system of three van der Pol oscillators (38)–(40).

As a check on the foregoing results obtained by perturbation methods, we offer the following results obtained by numerical integration of the system of three van der Pol oscillators (38)–(40). Figs. 10 and 11 show two different steady-state behaviors of Eqs. (38)–(40) for parameters $\epsilon = 0.1$, $\alpha = 1$, $\omega_1 = \omega_2 = \omega_3 = 1$. Both motions have the same amplitude, which is predicted to be $2\sqrt{1 + \alpha} = 2.828$, versus the actual amplitude from the data of Figs. 10 and 11, which is 2.824. Fig. 10 shows the clockwise mode which, as discussed earlier in this paper, is predicted to have a frequency of $\omega - \frac{\sqrt{3}}{2}\epsilon\alpha = 1 - 0.0866 = 0.9134$, i.e., a period of about 6.879.

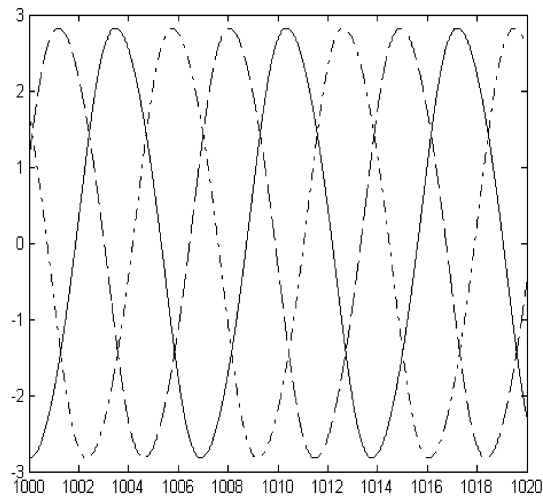


Fig. 10. Results of numerical integration of three van der Pol oscillators, Eqs. (38)–(40) for initial displacements $x(0) = 3$, $y(0) = 1$, $z(0) = 2$, with zero initial velocities. Time on horizontal axis omits t from 0 to 1000 to achieve steady state. Solid line = x , dot-dashed line = y , dashed line = z . Note that maxima occur in the order x, y, z , which represents a clockwise wave around Fig. 1.

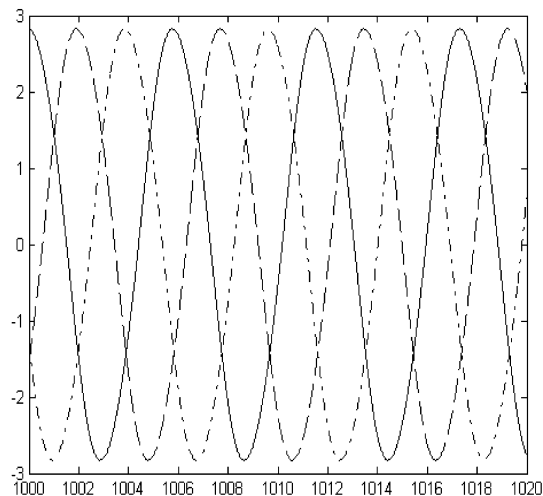


Fig. 11. Results of numerical integration of three van der Pol oscillators, Eqs. (38)–(40) for initial displacements $x(0) = 3$, $y(0) = 2$, $z(0) = 1$, with zero initial velocities. Time on horizontal axis omits t from 0 to 1000 to achieve steady state. Solid line = x , dot-dashed line = y , dashed line = z . Note that maxima occur in the order x, z, y , which represents a counterclockwise wave around Fig. 1.

The actual period, from the data of Fig. 10, is 6.870. Fig. 11 shows the counterclockwise mode, which is predicted to have a frequency of $\omega + \frac{\sqrt{3}}{2}\epsilon\alpha = 1.0866$, i.e., a period of about 5.782. The actual period, from the data of Fig. 11, is 5.775.

5. Conclusions

The goal of this work has been to investigate a system of three coupled limit cycle oscillators which exhibits two stable steady states. Each steady state represents a wave moving around the trio of oscillators in opposite directions. We investigated the existence, stability and bifurcation of such motions in a system of phase-only oscillators. This led us to a more realistic system of three van der Pol oscillators which was studied by using perturbation methods and confirmed by using numerical integration.

The ideal system of three identical oscillators was investigated for robustness in both phase-only and van der Pol models. In the case of phase-only oscillators, Fig. 5 shows the extent to which the frequencies of the individual oscillators can be detuned, and the system still function to have two stable steady states. Fig. 9 shows the comparable information when the system is taken as three van der Pol oscillators. Note the similarity of the shape of the stable regions in Figs. 5 and 9. In both cases, the greatest detuning stability occurs when two of the oscillators have the same frequencies, i.e. when $W_1 = W_2$ (Fig. 5) or $\Delta_1 = \Delta_2$ (Fig. 9). A basic difference between these cases is that stability is lost in Fig. 5 when one of the stable states disappears in a saddle-node bifurcation, whereas stability is lost in Fig. 9 when one of the stable states undergoes a supercritical Hopf bifurcation in which a stable limit cycle is born in the slow flow (which corresponds to a stable quasiperiodic motion in the original van der Pol oscillators).

Our motivation for studying this problem is to provide the theory for the design and construction of a machine which can be used to make decisions, a first step towards artificial intelligence. In particular we expect to see such applications in the area of MEMS.

Acknowledgements

This work was partially supported under the CMS NSF Grant CMS-0600174 “Nonlinear Dynamics of Coupled MEMS Oscillators”. The author L.M. acknowledges support from the Engineering College of Cornell University.

Appendix

For convenience in this section, the coefficients α_{ij} are written in the form aij . The coefficients in Eq. (8) are

$$c_1 = -\frac{a_{12}a_{31} + a_{13}a_{21} + a_{12}a_{13}}{a_{21}a_{32} + a_{21}a_{23} + a_{12}a_{23}} \quad (75)$$

$$c_2 = \frac{a_{21}\Omega_2 + a_{12}\Omega_1}{a_{21}a_{32} + a_{21}a_{23} + a_{12}a_{23}} \quad (76)$$

The coefficients K_i in Eq. (11) are all sums of terms of the form:

$$A(a_{12})^{i_1}(a_{13})^{i_2}(a_{21})^{i_3}(a_{23})^{i_4}(a_{31})^{i_5}(a_{32})^{i_6}(\Omega_1)^{i_7}(\Omega_2)^{i_8} \quad (77)$$

where $\sum_{j=1}^8 i_j = 8$ and where A is an integer. For example, K_0 consists of 38 terms, one of which is $8a_{12}a_{21}a_{23}^2\Omega_1^2\Omega_2^2$. The number of monomials in each K_i is as follows: K_0 has 38, K_1 has 76, K_2 has 165, K_3 has 200, K_4 has 183, K_5 has 50, and K_6 has 27, for a total of 739 terms.

The stability of the equilibria (63)–(65) are determined by computing the eigenvalues of the Jacobian matrix of Eqs. (52)–(56). In the case of (63), the real parts of the eigenvalues turn out to be

$$\left\{ \frac{3\alpha}{2}, \frac{3\alpha}{2}, \frac{7\alpha}{2} - 1, \frac{7\alpha}{2} - 1, 2\alpha - 1 \right\} \quad (78)$$

Since $\frac{3\alpha}{2} > 0$ for $\alpha > 0$, we see that (63) is unstable for $\alpha > 0$. In the case of equilibria 64 and 65, the situation is more complicated. Both of these equilibria turn out to have the same eigenvalues, one of which is $\lambda = -\alpha - 1$, which is stable for $\alpha > 0$, and four others which satisfy the following characteristic equation:

$$4\lambda^4 + (20\alpha + 8)\lambda^3 + (46\alpha^2 + 26\alpha + 4)\lambda^2 + (66\alpha^3 + 36\alpha^2 + 6\alpha)\lambda + 57\alpha^4 + 24\alpha^3 + 3\alpha^2 = 0 \quad (79)$$

To prove stability of this equation for $\alpha > 0$, we set $\lambda = \text{Re} + i\text{Im}$ and obtain two real equations by requiring real and imaginary parts to vanish. Then we use the MACSYMA/MAXIMA command ELIMINATE to eliminate Im and we obtain a single real equation on Re which turns out to be a polynomial of degree 16 having 143 terms, all coefficients of which are, however, non-negative for $\alpha > 0$. Thus by Descartes' rule of signs, there are no positive roots Re, and stability follows.

References

- [1] Hoppensteadt F, Izhikevich E. Oscillatory neurocomputers with dynamic connectivity. *Phys Rev Lett* 1999;82:2983–6.
- [2] Zhalalutdinov MK, Baldwin JW, Marcus MH, Reichenbach RB, Parpia JM, Houston BH. Two-dimensional array of coupled nanomechanical resonators. *Appl Phys Lett* 2006;88:143504.
- [3] Rand R, Wong J. Dynamics of four coupled phase-only oscillators. *Commun Nonlinear Sci Numer Simul*. [doi:10.1016/j.cnsns.2006.06.013](https://doi.org/10.1016/j.cnsns.2006.06.013).
- [4] Cohen AH, Holmes PJ, Rand RH. The nature of the coupling between segmental oscillators of the lamprey spinal generator for locomotion: a mathematical model. *J Math Biol* 1982;13:345–69.
- [5] Kuramoto Y. *Chemical oscillations, waves and turbulence*. Dover; 2003.
- [6] Nishiyama N, Eto K. Experimental study on three chemical oscillators coupled with time delay. *J Chem Phys* 1994;100:6977–8.
- [7] Ashwin P, King GP, Swift JW. Three identical oscillators with symmetric coupling. *Nonlinearity* 1990;3:585–601.
- [8] Cole JD. *Perturbation methods in applied mathematics*. Blaisdell Pub. Co.; 1968.
- [9] Nayfeh AH. *Perturbation methods*. Wiley; 1973.
- [10] Rand RH. Lecture notes on nonlinear vibrations (version 52). Available from: (<http://audiophile.tam.cornell.edu/randdocs/nlvibe52.pdf>); 2005.
- [11] Rompala K, Rand R, Howland H. Dynamics of three coupled van der Pol oscillators with application to circadian rhythms. *Commun Nonlinear Sci Numer Simulat* 2007;12:794–803.
- [12] Strogatz SH. *Nonlinear dynamics and chaos*. Addison-Wesley; 1994.